A Novel Approach to Identify the Drivers of Drought under Future Climate Change Scenario

Jagadish Padhiary
National Institute of Technology Rourkela
Kanhu Charan Patra
NIT Rourkela: National Institute of Technology Rourkela
Sonam Sandeep Dash (ssdash@yahoo.com)
University College Dublin https://orcid.org/0000-0003-1306-6925

Research Article

Keywords: Catchment, Climate Change, Drought, aSPEI, SPI, SPEI, SDI

Posted Date: March 21st, 2022

DOI: https://doi.org/10.21203/rs.3.rs-1419070/v1

Abstract

Climate change is one of the primary drivers that alters the natural balance of hydrologic cycle and leads to onset of hydrologic extreme situations. Among those extremes, drought is the most devasting and complex catchment hazard caused because of climate change. In this context, it is quite essential to study the implications of climatic and catchment alterations on different types of drought processes. The present study analyzed the Standardized Precipitation Index (SPI), Standardized Precipitation Evapotranspiration Index (SPEI), hydrological drought by Streamflow Drought Index (SRI), and Agricultural Standardized Precipitation Evapotranspiration Index (aSPEI) across multiple time scales of the future climate change scenarios. Further, this study attempted a correlation-based approach to identify the suitable drought index to characterize the agricultural drought and critical drought index estimates over the study region. The aSPEI is proved to be an improvement over the conventional SPEI for analyzing the agricultural drought characteristics. The 6-month time scale is found to be the most suitable reference period for drought monitoring with highest correlation estimate of 0.688 across all the three study regions. Individually, catchment and climate variables failed to represent the drought dynamics over the catchment, whereas the combined model adequately represented the drought dynamics over the study region. The relative impact of different process components revealed that the precipitation in the climate model and baseflow index in catchment model have significant impact on short-term drought prediction, while in the combined model, the baseflow index alone is sufficient. The methodology suggested herein could be adopted in any global catchment to represent the drought process, and subsequently, identifies the drivers of drought with utmost accuracy.

1 Introduction

Drought is a natural phenomenon that occurs due to reduced availability of water from normal conditions over the analysis period. Poor water management practices in large river basins lead to acute drought scenario; thereby affecting the stakeholders in an adverse manner (Dash et al., 2019). In the 21st century, significant alteration in climate causes potential environmental fallouts leading to many adverse societal consequences. As envisaged from the past climate change impact analysis studies, temperature is prone to increase at a faster rate than the anticipated rate during the twenty-first century (Gosain et al., 2011; Padhiary et al., 2020). This increase in temperature affects the global water cycle (Milly et al., 2002), which results in occurrence of extreme hydrological events. Variation of precipitation due to climate change may also accelerate the occurrence of extreme events such as drought and flood.

Drought is classified based on the deficiency of major hydro-climatic variables causing the phenomenon. Meteorological drought occurs due to a shortage of precipitation as compared to the normal precipitation of that area. The shortage of surface and sub-surface water from normal conditions causes hydrological drought. The deficit of soil moisture in the root zone of crop induces the origin of agricultural drought (Mishra and Singh, 2010). Meteorological drought can determine only the onset of drought, while the hydrological and agricultural drought reflects the different stages of drought development (Golian et al., 2015). Investigation of the causes, finding solutions, and subsequent, management are the important steps towards an amicable solution to this impending crisis of the 21st century. Among the commonly used meteorological drought indices, the standardized precipitation index (SPI) (McKee et al., 1993), which requires only the precipitation data (Dash et al., 2012) performs effectively under varying climatic conditions.

Different drought indices have been used widely to analyze the crop losses and identify drought impact on crop yield (Wang et al., 2016; Peña-Gallardo et al., 2019). For long-term studies, the simulated and satellite crop yield data are the only way outs as it is difficult to get accurate long-term crop yield information (Liu et al., 2015). For quantification of meteorological drought, relatively less complex indices such as the SPI (McKee et al., 1993), SPEI, and the Reconnaissance Drought Index (RDI) (Tsakiris et al., 2007) have been used extensively (Tigkas and Tsakiris, 2015). The SPI needs only precipitation data, whereas the SPEI or RDI includes both precipitation and potential evapotranspiration (*PET*) data. The advantage of SPEI over SPI includes (Dash et al., 2021): (1) the effect of temperature change in drought

characteristics and (2) useful for all climatic conditions with its usefulness to evaluate the climate change impact on drought under different future scenarios. For estimating *PET* in SPEI, the Penman-Monteith method (Begueria et al., 2014) is extensively used. The characteristic of hydrological drought has been widely analyzed in recent years using streamflow drought index (SDI) (Hong et al., 2015).

The representation of drought characteristics under a single factor is highly erroneous (Huang et al., 2015). The meteorological drought indices cannot represent the entire drought situation with utmost accuracy. They only express the characteristics of long-term droughts and also the entire water supply condition may not be determined. Therefore, the combined use of meteorological and hydrological drought indices can fulfill the gap and more comprehensive results can be inferred. Duration of hydrological drought affects the lives of the aquatic ecosystems, and its severity influences the availability of water for different purposes, i.e., agriculture, hydropower production, domestic purposes (Humphries and Baldwin, 2003). A hydrological drought is actuated by the variability of moisture in the atmosphere. It is influenced by both climate as well as catchment characteristics (Mishra and Singh, 2010; Van Loon, 2015); however, the challenge to understand the process that affects the drought event due to complex interaction between climate and catchment variables remained still unexplored. Hence, it is very important to identify the key variables which influence the hydrological drought phenomenon.

In light of the above discussions, the present study tries to answer the following research questions: i) What is the impact of climatic variables in governing the meteorological and hydrological drought phenomena?; ii) How does the interaction between climate and catchment process affect the drought onset?; and iii) What are the key variables governing the drought process in a region? Corresponding to this, the present study undertakes the following specific objectives: The impact of climate change on meteorological and hydrological droughts has been assessed. Moreover, the anthropogenic effect on hydrological droughts has also been analyzed.

2 Materials And Method

2.1 Study Area

The Anandapur catchment of Baitarani River Basin is situated between 85º0'0" to 86º30'0" E longitude and 21º0'0" to 22º30'0"N latitude. This catchment is selected as the study area due to the availability of its data and is not studied before. It can be located in the Keonjhar district of Odisha state, India (Fig. 1). The catchment area is 8645 km^2 with topographic elevation ranging from 32 to 1181 m above mean sea level (MSL). The basin experiences an undulated topography with an average slope varying between 0–2%. The average rainfall in the basin is 1628 mm with a sub-humid tropical climate predominating over the complete basin. As per the information of the India Meteorological Department, the basin experiences four climatic seasons in a year, i.e., winter (January and February), pre-monsoon (March-May), monsoon (June–September) and post-monsoon (October–December). About 80% of rainfall occurs during the monsoon spanning between June and September. Temperature in the catchment vary between 30 and 36 ºC during the summer and 16–17 ºC during winter. Two land-use types, i.e. forest and farmland are predominant in the catchment. Being an agriculture dominant basin, rice, maize, green gram, wheat, groundnut and vegetable are cultivated throughout the year.

Two climate model such as the National Centre for Meteorological Research-Climate Model Version 5.0 (CNRM-CM5.0) and Geophysical Fluid Dynamics Laboratory- Climate Model Version 3.0 (GFDL-CM3.0) models have been used under the Coordinated Regional Downscaling Experiment (CORDEX) for South Asia (http://cccr.tropmet.res.in/cordex/). These two models were selected based on the model evaluation works of Sperber et al. (2013) and Hasson et al. (2014). They found that CNRM-CM5.0 and GFDL-CM3.0 models simulate the June–September rainfall climatology more accurately over the Indian monsoon region. Hence, the CNRM-CM5.0 and GFDL-CM3.0 models of CMIP5 versions have been selected for this study.

2.2 Streamflow calibration and validation

The SWAT-CUP interface is coupled with SWAT model for the calibration and validation (Abbaspour et al., 2007) of daily discharge data. The Sequential Uncertainty Fitting (SUFI-2) algorithm is adopted for investigating the sensitivity and uncertainty in streamflow prediction. SWAT is calibrated and validated for monthly streamflow by comparing the results with the observed streamflow at the Anandapur outlet. Three years (1980–1982) are considered for the warm-up of the model, and subsequently, the period 1983–2003 and 2004–2012 are selected as calibration and validation periods, respectively.

Performance of the model is evaluated by checking the reliability of its output through various statistical indicators (Moriasi et al., 2007). In this study, the Nash–Sutcliffe efficiency (NSE) (Eq. 2), coefficient of determination (R^2) (Eq. 3) and percent bias (PBIAS) (Eq. 4) statistical indicators are used in the model performance evaluation. Performance of the model is good when the PBIAS is within ± 15%, NSE is above 0.75 (Moriasi et al., 2007) and R^2 is close to one. The following equations are used for evaluation of the statistical indicators:

$$NSE = 1 - \frac{\sum_{i=1}^{N}(O_i - S_i)^2}{\sum_{i=1}^{N}(O_i - \bar{O})^2}$$

1

$$R^2 = \left\{ \frac{\sum_{i=1}^{N}(O_i - \bar{O})(P_i - \bar{P})}{\left[\sum_{i=1}^{N}(O_i - \bar{O})^2\right]^{0.5}\left[\sum_{i=1}^{N}(P_i - \bar{P})^2\right]^{0.5}} \right\}^2$$

2

$$PBIAS = 100 * \frac{\sum_{i=1}^{t}(O_i - S_i)_i}{\sum_{i=1}^{t} O_i} \quad (3)$$

where O_i is the ith observed data, S_i the i^{th} predicted value, P_i the i^{th} predicted data, $\bar{O}$ the mean of measured data, $\bar{P}$ the mean of model estimated values, and N the total number of simulation periods.

Correlation analysis is commonly used to know the relationship between two variables (Ichii et al., 2002). Correlation between drought indices and decomposed crop yields are assessed using the Pearson correlation coefficient, which is calculated as follows:

$$r_{X,Y} = \frac{\sum\left(X - \bar{X}\right)\left(Y - \bar{Y}\right)}{\sqrt{\sum\left(X - \bar{X}\right)^2 \sum\left(Y - \bar{Y}\right)^2}}$$

4

where X and Y are the time series of two variables, $\bar{X}$ and $\bar{Y}$ are the mean values of the two series. The correlation coefficient $r_{X,Y}$ ranges from − 1 to + 1, with − 1 indicating that the two variables are perfectly negatively correlated and + 1 indicating a perfect positive correlation.

2.3 Bias Correction and Downscaling

The bias correction of GCM output is essential due to the associated systematic and random model errors (Teutschbein and Seibert, 2013; Fiseha et al., 2014). The parametric and non-parametric bias correction techniques are generally used for reducing the bias from GCM output. But non-parametric bias correction technique has used in this study for efficient reduction of bias from GCM outputs (Gudmundsson et al., 2012). The non-parametric quantile mapping bias correction method is based on following Equation.

$$P_{obs} = F_{obs}^{-1}\left(F_{wet}\left(P_{wet}\right)\right)$$

5

where, P_{obs} and P_{wet} are the observed and weighted precipitation, F_{wet} the CDF of P_{wet} and F_{obs}^{-1} the inverse CDF corresponding to P_{obs}.

A multi-GCM ensemble approach is used in this study because a single GCM output is not reliable enough in evaluating future climate change impacts. A weighted ensemble average approach is used to ensemble the two GCMs (CNRM-CM5.0 and GFDL-CM3.0).

2.4 Estimation of Drought Indices

2.4.1 Standardized Precipitation Index (SPI)

The SPI method was proposed by Mckee et al. (1993, 1995) to assess and analyse the meteorological drought. The SPI can be used to identify the drought conditions for different time scales (3-, 6-, 12-, 24- and 48-month time scales); therefore, it is used to compare drought conditions among different time periods and regions with different climatic conditions. In the SPI computation, only normally or log-normally distributed input data can be used. But precipitation data distribution is not normally distributed, rather it follows the gamma distribution. Hence, the data must be transformed to normal distribution before they can be used for computation of the SPI. The SPI computation is a probability transformation of observed precipitation series to the standard normal distribution having standard deviation one and mean zero (Mckee et al. 1993). A Positive SPI values indicate wet periods, while negative values indicate drought periods (Dash et al. 2021). The computation of SPI consists of the following steps:

1) For the computation of SPI gamma distribution is fitted to the observed precipitation data. The gamma probability distribution function is expressed as:

$$g(x) = \frac{1}{\beta^{\alpha}\Gamma(\alpha)} x^{\alpha-1} e^{-x/\beta}$$

6

where α > 0 is a shape parameter, β > 0 is a scale parameter, and x > 0 is the amount ofprecipitation. Γ(α) is the gamma function, which is defined as:

$$\Gamma(\alpha) = \int_0^{\infty} y^{\alpha-1} e^{-y} dy$$

7
Fitting the distribution to the data requires estimation of α and β. These parameters can be estimated as follows:

$$\alpha = \frac{1}{4A}\left(1 + \sqrt{1 + \frac{4A}{3}}\right), \beta = \frac{\bar{x}}{\alpha}, \text{with } A = \ln \bar{x} - \frac{\sum \ln(x)}{n} \quad (8)$$

where n is number of observed precipitations and x refers to the mean of the sample data.

Integrating the probability density function with respect to x yields the following expression G(x) for the cumulative probability:

$$G(x) = \int_0^x g(x)\,dx = \frac{1}{\beta^{\alpha}\Gamma(\alpha)} \int_0^x x^{\alpha-1} e^{-x/\beta} dx$$

9
The gamma distribution is undefined for x = 0; however, it is possible to have several zero values in a sample set. Therefore, in order to account for zero value probability, the cumulative probability function for gamma distribution is modified as:

$$H(x) = q + (1 - q)\,G(x)$$

10
where q is the probability of zero precipitation.

2) The cumulative probability distribution is transformed into the standard normal distribution and the transformed probability distribution is considered as SPI (Abramowitz and Stegun 1964).

$$SPI = -\left(t - \frac{c_0 + c_1 t + c_2 t^2}{1 + d_1 t + d_2 t^2 + d_3 t^3}\right), t = \sqrt{\ln \frac{1}{(H(x))^2}} \quad (11)$$

For$0 < H(x) < 0.5$

$$SPI = +\left(t - \frac{c_0 + c_1 t + c_2 t^2}{1 + d_1 t + d_2 t^2 + d_3 t^3}\right), t = \sqrt{\ln\left(\frac{1}{(1.0 - H(x))^2}\right)} \quad (12)$$

2.4.2 Standardized Precipitation Evapotranspiration Index (SPEI)

The Standardized Precipitation Evapotranspiration Index (SPEI) is an extension of the conventional SPI, which is used for assessing the temperature-induced moisture stress (Chitsaz and Hosseini-Moghari, 2018). The drought classification of SPEI is almost similar to the SPI based drought classification system given by McKee et al. 1993. The steps for estimation of SPEI could be adopted from the method given by Vicente-Serrano et al., 2010.

2.4.3 Streamflow Drought Index (SDI)

The SDI was proposed by Nalbantis (2008) for analysis of hydrological drought characteristics at different time scales. The calculation steps include: (1) Accumulation of the monthly simulated streamflow data, (2) Fitting Gamma probability distribution to these accumulated streamflow time series, (3) Estimation of cumulative density function of observed cumulative streamflow data, and finally, (4) The cumulative probability is transformed to a normal distribution with mean

zero and standard deviation one. The SDI is evaluated based on the monthly standard normal flow (Nalbantis and Tsakiris 2009). The calculation procedure is similar to SPI except that discharge monthly series were used instead of rainfall data as the input in SDI. The cumulative streamflow volume could be obtained as given below:

$$V_{i,k} = \sum_{j=1}^{3k} Q_{i,j} i = 1, 2, 3.... ; j = 1, 2, ... , 12; k = 1, 2, 3, 4$$

13

where $V_{i,k}$ is the cumulative streamflow value of i^{th} hydrological year and the k^{th} reference period, $Q_{i,j}$ is the monthly streamflow, *j* denotes the month within the hydrological year.

The SDI is defined as by:

$$SDI_{i,k} = \frac{V_{i.k} - \bar{V}_k}{s_k}$$

14

where, $\bar{V}_k$ and s_k are respectively the mean and standard deviation of cumulative streamflow volumes of reference period k.

Usually, Gamma and log-normal distributions are used for representing streamflow. However, in case of log-normal distribution, the normalization is relatively easier. The SDI is defined as:

$$SDI_{i,k} = \frac{y_{i,k} - \bar{y}_k}{s_{y,k}}, i = 1, 2, ...; k = 1, 2, 3, 4 \text{ (15)}$$

$$y_k = \ln\left(V_{i,k}\right), i = 1, 2, ...; k = 1, 2, 3, 4 \text{ (16)}$$

where, y_k is the natural logarithm of cumulative streamflow with mean $\bar{y}_k$ and the standard deviation $s_{y,k}$. SDI also has same drought-severity classes as those for SPI and SPEI.

2.4.4 Agricultural Standardized Precipitation Evapotranspiration Index (aSPEI)

In the aSPEI, effective precipitation is used instead of the total precipitation of the conventional SPEI. Though SPEI is found to be good for agricultural drought characterization (Fu et al., 2019), the use of effective precipitation leads to giving more promising results. Effective precipitation is evaluated to analyze agricultural drought characteristics for the concerned time scale. The term effective precipitation (P_e) has several definitions in different research fields (i.e., reservoir management, groundwater management, agricultural applications). In reservoir management, P_e is the amount of water from the total precipitation entering into the reservoir. In groundwater management, P_e is the portion of precipitation that contributes to groundwater recharge. Similarly, for agricultural applications, P_e is the percentage of precipitation that used by plant root for plat development. Here P_e is used in term water that contributes to the plant for consumptive use. In this study P_e is estimated using the CROPWAT model and the monthly total precipitation is used as the input variable (Smith, 1992), as given by:

$$P_e = P \times (125 - 0.2 \times P) / 125 \text{ For P} \leq 250\text{mm (17)}$$

$P_e = 0.1 \times P + 125$ For P > 250mm (18)

2.5 Selection of Appropriate Reference Period

Selection of the base periods for calculation of the agricultural drought index is based on the crop development time. For assessment of agricultural drought, the month of seeding is considered as the reference period. The reference period corresponding to various critical development stages of the plants is to know the early drought warning time. Short reference periods are more suitable for soil moisture condition, while long reference periods are appropriate for arid or semi-arid regions due to high percentage of zero precipitation values in the time series (Quiring and Ganesh 2010; Mallya et al. 2013). Generally, the crop development pattern follows seasonal weather variability. Therefore, the reference period should be selected according to crop development stages. For hydrological drought monitoring, the reference period starts from the first month of the hydrological year, while the first month of crop production is considered as starting of reference period for agricultural drought monitoring (Nalbantis and Tsakiris 2009).

The backward stepwise selection is performed to investigate the combined influence of climate, catchment variables on hydrological drought duration. The proposed backward stepwise selection model was evaluated based on the Akaike Information Criterion (AIC).

Backward stepwise selection (or backward elimination) is a variable selection method which:

i. Begins with a model that contains all variables under consideration (called the Full Model)

ii. Then starts removing the least significant variables one after the other
iii. The removal should continue until a pre-specified stopping rule is reached or no variable is left in the model
The least significant variable is treated as a variable that:

i. Has the highest p-value in the model, or

ii. Its elimination from the model causes the lowest drop in R^2, or
iii. Its elimination from the model causes the lowest increase in RSS (Residuals Sum of Squares) compared to other predictors
Finally the stopping rule criteria is defined in order to stop the algorithm. The stopping rule is satisfied when all remaining variables in the model have a p-value smaller than some pre-specified threshold. When that state is reached, backward elimination will terminate and return the current step's model. The threshold is determined by using Akaike Information Criterion (AIC) (Akaike, 1974).

3 Results And Discussion

3.1 Model Calibration and Sensitivity Analysis

In the early stage of calibration, sensitivity analysis for streamflow has been conducted at the monthly time-step using SWAT-CUP. Two indicators, *t-stat* and *p-value* are used for performing the sensitivity analysis. The *t-stat* represents measure of sensitivity, whereas the significance of sensitivity is assessed by the *p-value*. Parameters involved in the simulation of monthly streamflow and their final fitted values are listed in Table 1. The sensitivity of the parameters is quantified according to the ranking of the parameters. It can be seen from the table that parameters like ALPHA_BF, CH_K2, CH_N2 and SURLAG are more sensitive than other calibration parameters for streamflow simulation.

Table 1
SWAT parameters and their ranges during calibration for streamflow simulation

Sl. No.	Parameter	Description	Fitted Value	t-Stat	P-Value
1	v__ALPHA_BF.gw	Base flow recession alpha factor (days)	0.04	34.32	0.00
2	v__CH_K2.rte	Channel effective hydraulic conductivity (mm/h)	0.29	-4.70	0.00
3	v__CH_N2.rte	Manning's n value for the main channel	286.0	-1.95	0.05
4	v__SURLAG. bsn	Surface runoff lag time (day)	2690.8	1.06	0.28
5	r__SOL_AWC. sol	Available water capacity (mm/mm)	0.09	-0.74	0.45
6	v__ESCO. hru	Soil evaporation compensation factor	3.06	0.69	0.48
7	a__GW_DELAY.gw	Groundwater delay (day)	97.2	-0.58	0.55
8	a__GWQMN.gw	Threshold water depth in the shallow aquifer required for return flow to occur (mm)	0.31	0.52	0.59
9	r__SOL_K. sol	Saturated hydraulic conductivity (mm/h)	-0.05	-0.26	0.79
10	r__CN2.mgt	Soil Conservation Service curve number for AMC II	0.09	-0.05	0.95

*v_ means the existing parameter value is to be replaced by a given value, *a_ stands for a given value that is added to the existing parameter value, *r_ means that an existing parameter value is multiplied by 1 + the given value.

3.2 model performance and uncertainty analysis under present and future climate change scenario

The measured and simulated streamflow for both calibration and validation has a similar trend at the Anandapur gauging station. The *P* and *R* factors of model uncertainty analysis are found to be 0.84 and 0.87, respectively during the calibration and 0.70 and 0.69, respectively during the validation, which indicates that the model performance is satisfactory during both calibration and validation periods. The values of NSE, R^2, and PBIAS during calibration are 0.91, 0.92 and − 1.9 respectively, while they become 0.96, 0.97, and − 0.2 during the validation period respectively. However, for most of the times, underestimation is more profound during the simulation process. During the monsoon months of the years 2000, 2007 and 2008, significant underestimation is observed. Acceptable values of the goodness of fit statistics and similar temporal behavior between observed and simulated streamflow values indicate that the performance of the model is quite adequate and can be used for impact analysis study in the concerned study location.

The projected future precipitation and temperature variables so obtained are used as input to the validated SWAT model for simulating the hydrological fluxes for future time horizon. The future streamflow and evapotranspiration (ET) are simulated for the periods 2020–2035 and 2036–2050 for both RCP 4.5 and 8.5 scenarios and compared with base period (Table 2). From the seasonal analysis it can be envisaged that the streamflow is decreasing in monsoon season and increasing in all other seasons for both the future time periods. A relatively more decreased scenario for streamflow is observed for the period 2036–2050 as compared to the period 2020–2035 in the monsoon period across all the RCPs. The seasonal analysis of streamflow indicates that the streamflow magnitude in the base monsoon period is shifting towards the non-monsoon periods in the future time horizons. Conversely, ET is increasing across all the seasons of both the future time periods as compared to base period. The decrease in ET is more prevalent for the time period 2036–2050 across all the seasons as compared to the 2020–2035 time period. Unlike streamflow, the ET does not exhibit any seasonal shift between the base and future periods.

Table 2
Seasonal streamflow and evapotranspiration (ET) in the Anandapur catchment during the baseline and future climate change scenario.

Season	Base Period	RCP4.5		RCP 8.5		Base Period	RCP 4.5		RCP 8.5	
	Streamflow (m3/sec)	2020–2035	2036–2050	2020–2035	2036–2050	ET (mm)	2020–2035	2036–2050	2020–2035	2036–2050
winter	11.17	21.67	28.95	23.41	23.11	57.16	117.21	116.07	119.41	113.09
Pre-monsoon	18.35	32.74	29.31	28.91	31.71	308.71	325.12	315.11	335.05	313.31
Monsoon	616.8	577.88	565.91	606.92	513.09	467.67	474.54	482.41	479.28	478.51
Post-monsoon	96.72	141.32	98.89	143.96	164.62	153.86	193.83	194.67	198.54	192.32

3.3 Meteorological Drought Analysis

The SPI and SPEI drought events vary from mild to severe conditions for the analyzed years at all the four grid points as shown in Fig. 2. In Grid 1, the years 2030–2034, 2035, 2037, 2040 and 2043 are identified as mild to moderate drought years. Similarly, the Grid 2 shows mild to moderate drought during the years 2026-27, 2030-32, 2035-36, 2040, 2042-43 and 2045. Conversely, the years 2030-34, 2036, 2040-44 are observed as mild to moderate drought period in Grid 3 and the years 2026-27, 2030 -32, 2036, 2038, 2041, 2043 and 2046 are mild to moderate drought years in Grid 4. The numbers of mild and moderate drought months are predicted to be high by the SPEI as compared to the SPI, by considering both precipitation and temperature inputs. However, more numbers of severe drought months have been noticed by the SPI than the SPEI. The severe drought months could have increased because of the consideration of lowering in precipitation by the SPI.

The correlation between crop yield (Y) and the drought as estimated by the SPEI and aSPEI is evaluated by considering different reference periods for the Anandapur, Swampatana, and Champua locations of the study area (Table 3). The time scales of the drought analysis are linked to cropping periods of different crops. However, the periods at 1-, 3-, and 6-month are given more importance, since these periods are usually considered for quantification of agricultural drought. As the 12-month time period is larger than the general crop growing period, the time scale was neglected for the analysis of agricultural drought.

Table 3
Correlation coefficients (*r*) between annual crop yield (*Y*), SPEI and aSPEI for various reference periods in each study region

Time scales	Reference periods	Anandapur		Swampatana		Champua	
		SPEI	(aSPEI)	SPEI	(aSPEI)	SPEI	(aSPEI)
12 months	Oct–Sep	0.585	0.579	0.556	0.568	0.474	0.537
6 months	Oct–Mar	0.531	0.598	0.436	0.467	0.425	0.462
	Nov–Apr	0.547	0.589	0.528	0.551	0.548	0.559
	Dec–May	0.638	**0.688**	0.518	0.664	0.538	0.554
	Jan–Jun	0.531	0.577	0.528	0.564	0.428	0.493
3 months	Nov–Jan	0.353	0.419	0.316	0.372	0.237	0.257
	Dec–Feb	0.577	0.622	0.546	0.567	0.326	0.361
	Jan–Mar	0.551	0.603	0.543	0.576	0.438	0.450
	Feb–Apr	0.571	0.638	0.524	0.622	0.573	0.591
1 month	Nov	0.118	0.128	0.105	0.114	0.101	0.109
	Dec	0.412	0.428	0.315	0.353	0.272	0.291
	Jan	0.412	0.423	0.363	0.372	0.227	0.256
	Feb	0.415	0.447	0.345	0.364	0.249	0.283
	Mar	0.479	0.492	0.325	0.353	0.223	0.236
	Apr	0.431	0.442	0.322	0.331	0.236	0.258

The monthly time steps considered are 1-, 3-, and 6-month references within the cropping periods which helps to analyze the drought variation in different stages of crop growth. From the correlation results presented in Table 3, it has been observed that for most of the cases, the performance of aSPEI is better than SPEI and the 6-month reference period is most suitable for drought finding that has the highest correlation coefficient of 0.688 across all the regions. Conversely, a 3-month reference period gives higher correlation value corresponding to critical crop development periods and varies slightly from region to region due to variation in specific climatic conditions. The monthly reference period shows that the months of February, March, and April are more critical to drought conditions and the months November, December, and May are not so significant to drought conditions over the study region.

The correlation between crop yield and 6-month aSPEI based drought indices are shown in Fig. 3. The main aim of analyzing the relationship is to recognize the crop yield pattern with drought indices in the three study locations. The relationship indicates that the crop yield increases as the drought period attends wet spell and yield decreases as drought reaches to the warm/hot phase. The critical points in ($aSPEI_c$) are evaluated from the intersection point of the regression line and the X-axis, which indicates the resistance of crops to the drought in different study locations, and it is highly variable across the spatial domain. For Anandapur location, the average value of $aSPEI_c$ is -0.88, (Fig. 3a), which corresponds to the fact that the crop yield is affected due to climatic conditions as (aSPEI) reach to -0.88. Similarly, in the Swampatana and Champua locations, the crop yield is negatively affected when aSPEI reaches − 1.18 (Fig. 3b) and − 1.45 (Fig. 3c), respectively indicating relatively improved drought resistance regions.

Certainly, the effect of drought is different for different stages of cropping periods and regions as the drought is mainly affected by local climatic factors and management of water (Geng et al., 2016). Hence the critical drought index varies for different locations though the cropping is similar in the three chosen locations. Further, the future drought events are identified, which have a negative impact on crop yield by considering critical drought point of different regions as shown in Fig. 4. The red line in Fig. 4 represents the critical point line wherein, the drought index of the years which comes below the line represents the critical drought years where the crop yield decreases significantly. From 2030–2050, there is a high-risk involving loss in crop production for both the scenarios (RCP 4.5 and RCP 8.5) in all the three study locations. Hence, both the availability of water resources and crop management measures are required to be undertaken for both the periods and for all the regions.

3.4 Relationship between Meteorological and Hydrological Drought

Correlation coefficient between SPI and SRI is computed for the catchments at the 1-, 3-, 6-, and 12-month timescales covering the period from 2020 to 2050. The correlation coefficient between SPI and SRI varies in the range of 0.69–0.92, 0.76–0.94, 0.85–0.95 and 0.87–0.98 for 1-, 3-, 6-, and 12-month scales respectively. The correlation increases from 1-month timescale to 12-month timescale, which suggests that the SPI can be used as a substitute for the SDI to represent the hydrological drought at the longer timescale (e.g., 12-month or longer). Hence, particularly at long timescale, the changes in precipitation are directly responsible for causing changes in runoff.

3.5 Effect of Climate and Catchment on Hydrological Drought

3.5.1 Spatial Pattern of Key Climate and Catchment Variables

The spatial pattern of hydrological drought in a catchment is likely to be influenced by spatial variation of catchment and climate variables. Hence, it is essential to analyze the spatial variation of important variables, which are more sensitive to hydrological drought characteristics. A boxplot of climate variables (annual and seasonal precipitation) and catchment variables (baseflow index, crop land, and forest land) are shown in Fig. 5. The annual precipitation varies in the range of 1922–2275 mm, and in seasonal-scale the precipitation during spring, summer, and post-monsoon periods varies between 200–230 mm, 440–470 mm, and 400–420 mm respectively (Fig. 5a).

Spatial distribution of mean annual precipitation in the catchment is shown in Fig. 5a, b for the period 2020–2050. The mean annual precipitation is higher in the lower regions of the catchment. The spatial pattern of precipitation in a catchment influences the hydrological drought (Tran et al., 2015). When precipitation in a catchment decreases below the mean value, then meteorological drought occurs, which further leads to hydrological drought (Mishra and Singh, 2010). The spatial distribution of seasonal precipitation in the catchment revealed that the higher seasonal precipitation can be noticed in the downstream parts of the catchment during the post-monsoon, spring, and summer seasons.

Variation of catchment variables in the catchment, such as the baseflow index (BFI), cropland, and forestland is shown in Fig. 5b. BFI varies in the range of 0.32 to 0.44 for the sub-basin located in the Anandapur catchment. The BFI is associated with groundwater that contributes to streamflow. Total streamflow is contributed by baseflow during the dry season (Smakhtin, 2001). The BFI is influenced by the storage capacity and geological characteristics of a catchment (Bloomfield et al., 2009). The catchment variables linked to land use classes such as cropland and forest coverage vary from 0.41 to 0. 84, and 0.03 to 0.52, respectively in the catchment. These catchment variables are expressed as the ratio between the areas of land use class to the total area of the catchment. Land use is an important factor to control the hydrological drought in a catchment, e.g., the evapotranspiration increases and water yield reduces in the cropping areas (Zhang et al., 2016). Hence, more agricultural land coverage increases the hydrological drought in a catchment.

3.5.2 Potential Influence of Climate and Catchment Variables

The effect of climate and catchment variables on short (SDI 1), medium (SDI 6), and long (SDI 12) term hydrological drought is evaluated separately using linear regression. These individual models are named as climate and catchment models (Table 4). Finally, the combined effect of climate and catchment variables on hydrological drought characteristics is assessed using backward stepwise selection approach. This integrated model is named as the combined model. The drought classes are described through the climate and catchment variables and the result are estimated through p and R^2 estimates.

Table 4
Model performance based on the climate variables (Climate model), catchment variables (Catchment model) and combination of the variables (Combined model)

Performance based on only climate variables (Climate model)			
Drought class	Variable	p-value	R^2
SDI 1	Mean annual precipitation	0.00231 (**)	0.20
	Annual evapotranspiration	0.01034 (*)	
SDI 6	Summer precipitation	0.0062 (***)	0.25
SDI 12	Summer precipitation	0.0465 (*)	0.07
Performance based on only catchment variables (Catchment model)			
Drought class	Variable	p-value	R^2
SDI 1	Pastureland	0.004418 (**)	0.51
	BFI	0.000345 (***)	
SDI 6	Pasture	0.00000974 (***)	0.45
SDI 12	Pasture	0.0416 (*)	0.09
	BFI	0.000347 (***)	
Performance based on combination of the variables (Combined model)			
Drought class	Variable	p-value	R^2
SDI 1	Pastureland	0.0040 (**)	0.61
	BFI	0.00000041 (***)	
	Mean annual precipitation	0.0087 (**)	
SDI 6	Pasture	0.000843 (***)	0.49
	Spring precipitation	0.000000813 (***)	
SDI 12	Summer precipitation	0.000301 (***)	0.20
	Pastureland	0.0416 (*)	
	BFI	0.0347 (**)	

Star (*) indicates the significant level. The single star (*) implies less significant whereas, triple star (***) indicates more significant value.

3.5.3 Potential Influence on Short Term Drought

The climate change impact on hydrological drought over a river basin has been analysed by many researchers (Wang et al., 2015; Sheffield et al., 2012). As envisaged from Table 4, the climate variables, such as the mean annual precipitation (A.PCP) and annual evapotranspiration (A.ET) have significant impact on short-term hydrological drought duration in the Anandapur catchment. Among the two climate variables, i.e., A.PCP and A.ET, the mean annual precipitation shows higher significant value (p-value = 0.00231) which indicates that precipitation have comparatively higher influence on the hydrological drought duration than the evapotranspiration. Therefore, the short-term drought occurs in the catchment when the precipitation attends below the normal value.

Next to precipitation, the evapotranspiration has significant control on the short-term hydrological drought in the climate change scenario. This condition further leads to supplementary loss of water stored in the catchment. Thus, the possibility of hydrological drought may increase by combining the low precipitation and high evapotranspiration estimates. The coefficient of determination (R^2) values as produced by the climate model is 0.20 (Table 4) while determining the short-term drought duration. This shows that climate variable cannot determine the short-term drought with reasonable accuracy. In case of catchment model, the BFI is the most significant catchment variable (p-value = 0.000345) for evaluating the short-term drought duration (Table 4). In this case, the significance value of R^2 (= 0.51) indicates that the catchment variables have more significant control on short-term drought than the climate variables.

The baseflow has strong role in controlling hydrological drought in a catchment. Therefore, information regarding the baseflow is important for water resources management in a catchment during the drought periods (Smakhtin, 2001). Apart from BFI, the other catchment variable, such as the pastureland has a major role in controlling short-term hydrological drought (Table 4, p-value = 0.004418). In the cropping areas, the evapotranspiration increases, which reduces the contribution of streamflow from the cropland. This leads to decrease in the water yield and resulted in increased hydrological drought (Bagley et al., 2014).

Effect of both, the climate and catchment variables on hydrological drought duration is analysed using the backward step selection method. Five variables from both climate and catchment considerations are used in the combined model for evaluation of hydrological drought duration as detailed in Table 4. In the combined model, the R^2 value is obtained as 0.61 for evaluation of short-term drought, which indicates that the combination of climate and catchment variables significantly improved the prediction of hydrological drought duration in the catchment. The BFI has the most significant control (p-value = 0.00000041) on short-term hydrological drought among all the variables in the combined model.

3.5.4 Potential Influence on Medium- and Long-Term Drought

The effect of climate and catchment variables on medium- and long-term drought duration has been analysed in this section. The summer precipitation (PCP.SUM) and Pastureland (cropland) have significant control on medium-term drought duration in the catchment. In this case, the catchment variable shows higher significant control on hydrological drought than climatic variable with higher $R^2$of 0.45. Similarly, the combined model shows the value of R^2 as 0.49 for medium-term drought duration, which indicates improvement of the performance of model with addition of catchment variables with the climate variables. The spring precipitation (PCP.SPN) shows most significant control (p-value = 0.000000813) on medium-term drought in the combined model. Following the spring precipitation, the cropland is the next significant (p-value = 0.000843) catchment variable responsible for medium-term drought.

In the climate model, summer precipitation (PCP.SUM) is the only climate variable that has the potential impact (p-value = 0.0465) on long-term drought (Table 4). Similarly, the BFI has the significant impact (p-value = 0.000347) on long-term hydrological drought in the catchment model. Among the climate and catchment variables, the summer precipitation has significant control (p-value = 0.000301) on long-term hydrological drought in the combined model. From the above analysis, it can be envisaged that the climate and catchment models are competent to predict the short- and medium-term drought duration. However, the climate and catchment variables have less correlation with long-term drought than

the short- and medium-term drought. The result also indicates that the influence of catchment variables on hydrological drought over the catchment is higher as compared to the climate variables.

4 Conclusion

Onset of drought in a catchment is analyzed by considering different existing and advances drought indices. It has been observed that a catchment is subjected to multiple drought conditions. The meteorological drought is analyzed under SPI and SPEI drought indices estimates. The variation of SPI and SPEI are almost similar in annual time scale. The severe drought months increases under SPI, while temperature effects the variation of mild- and moderate-drought events under the SPEI scenario. The agricultural standardized precipitation evapotranspiration index (aSPEI) is used as an improvement over the conventional SPEI for analyzing the agricultural drought characteristics. From the correlation analysis, it is envisaged that the performance of aSPEI is better than SPEI, and the 6-month reference period is the most suitable for drought monitoring with higher correlation estimate of 0.688 across all regions. The future drought events are identified which have a negative impact on crop yield by considering critical drought point for different regions.

The correlation between SPI and SDI is evaluated for different timescales. Larger correlation is observed at longer timescale, which suggests that SPI can be used as a substitute of SDI to represent the hydrological drought at the long-term scale. The climate model, which is based on the climate variables is not adequate enough to predict hydrological drought scenario in the catchment. Performance of the model improves substantially by the combination of catchment variables and climate variables. Precipitation in the climate model and baseflow index in catchment model have significant impact on short-term drought prediction, while in the combined model, the baseflow index alone is proved significant. The spring precipitation has significant influence on medium-term drought whereas, the summer precipitation shows higher influence for long-term drought.

Declarations

Acknowledgement

The authors feel grateful to the IMD, Bhubaneswar and CWC, Bhubaneswar for providing necessary hydro-meteorological data used in this study.

Author Contributions

J Padhiary: Software, Methodology, Analysis, Writing original draft

K C Patra: Conceptualization, Reviewing and editing Original Draft

S S Dash: Conceptualization, Analysis, Reviewing and editing Original Draft

Funding

The authors declare that no funds, grants, or other supports were received during the preparation of this paper.

Data Availability

The data used in this paper can be obtained from the corresponding author with prior request.

Ethical Approval

This paper has neither been published nor been under review for publication elsewhere.

Consent to Participate

The authors have participated in the preparation and submission of this paper for publication in the Water Resources Management.

Consent to Publish

The authors would like to publish their paper in Water Resources Management.

Competing Interests

The authors have no relevant fnancial or non-fnancial interests to disclose, and they have no conflicts of interest to declare that are relevant to the content of this paper and its publication.

References

1. Abbaspour KC, Vejdani M, Haghighat S, Yang J (2007) SWAT-CUP calibration and uncertainty programs for SWAT. MODSIM 2007 international congress on modelling and simulation, modelling and simulation society of Australia and New Zealand,1596–1602
2. Abramowitz M, Stegun IA (1964) Handbook of mathematical functions with formulas, graphs, and mathematical tables. US Government printing office
3. Allen RG (1986) A Penman for all seasons. J Irrig Drain Eng 112(4):348–368
4. Arnold JG, Srinivasan R, Muttiah RS, Williams JR (1998) Large area hydrologic modeling and assessment part I: model development 1. J Am Water Resour Assoc Wiley Online Library 34(1):73–89
5. Bagley JE, Desai AR, Harding KJ, Snyder PK, Foley JA (2014) Drought and deforestation: has land cover change influenced recent precipitation extremes in the Amazon? J Clim 27:345–361
6. Begueria S, Vicente-Serrano SM, Reig F, Latorre B (2014) Standardized precipitation evapotranspiration index (SPEI) revisited: parameter fitting, evapotranspiration models, tools, datasets and drought monitoring. Int J Climatol Wiley Online Library 34(10):3001–3023
7. Bloomfield JP, Allen DJ, Griffiths KJ (2009) Examining geological controls on baseflow index (BFI) using regression analysis: An illustration from the Thames Basin, UK. J Hydrol 373:164–176
8. Bouraoui F, Benabdallah S, Jrad A, Bidoglio G (2005) Application of the SWAT model on the Medjerda river basin (Tunisia). Phys Chem Earth, Parts A/B/C, Elsevier, 30(8–10), 497–507
9. Chandra R, Saha U, Mujumdar PP (2015) Model and parameter uncertainty in IDF relationships under climate change. Adv Water Resour 79:127–139
10. Chitsaz N, Hosseini-Moghari S-M (2018) Introduction of new datasets of drought indices based on multivariate methods in semi-arid regions. Hydrol Res 49:266–280
11. Dash BK, Rafiuddin M, Khanam F, Islam MN (2012) Characteristics of meteorological drought in Bangladesh. Nat hazards 64:1461–1474
12. Dash SS, Sahoo B, Raghuwanshi NS (2019) A SWAT-Copula based approach for monitoring and assessment of drought propagation in an irrigation command. Ecol Eng 127:417–430
13. Dash SS, Sahoo B, Raghuwanshi NS (2021) How reliable are the evapotranspiration estimates by Soil and Water Assessment Tool (SWAT) and Variable Infiltration Capacity (VIC) models for catchment-scale drought assessment and irrigation planning? J Hydrol 592:125838
14. Ficklin DL, Stewart IT, Maurer EP (2013) Effects of projected climate change on the hydrology in the Mono Lake Basin, California. Clim Change, vol 116. Springer, pp 111–131. 1

15. Fiseha BM, Setegn SG, Melesse AM, Volpi E, Fiori A (2014) Impact of climate change on the hydrology of upper Tiber River Basin using bias corrected regional climate model. Water Resour. Manag., Springer, 28(5), 1327–1343
16. Fu J, Niu J, Kang S, Adeloye AJ, Du T (2019) Crop production in the Hexi Corridor challenged by future climate change. J Hydrol 579:124197
17. Geng G, Wu J, Wang Q, Lei T, He B, Li X, Mo X, Luo H, Zhou H, Liu D (2016) Agricultural drought hazard analysis during 1980–2008: a global perspective. Int J Climatol 36:389–399
18. Giorgi F, Mearns LO (2002) Calculation of average, uncertainty range, and reliability of regional climate change from AOGCM simulations via the reliability ensemble averaging (REA) method. J Clim 15:1141–1158
19. Golian S, Mazdiyasni O, AghaKouchak A (2015) Trends in meteorological and agricultural droughts in Iran. Theor Appl Climatol 119:679–688
20. Gosain AK, Rao S, Arora A (2011) Climate change impact assessment of water resources of India.Curr. Sci.356–371
21. Gudmundsson, L., Bremnes, J. B., Haugen, J. E., and Engen-Skaugen, T., 2012. Technical note: downscaling RCM precipitation to the station scale using statistical transformations& dash; a comparison of methods. Hydrol. Earth Syst. Sci., 16, 3383–3390
22. Hasson S, Lucarini V, Pascale S, Böhner J (2014) Seasonality of the hydrological cycle in major South and Southeast Asian river basins as simulated by PCMDI/CMIP3 experiments. Earth Syst Dyn 5(1):67–87
23. Heim RR Jr (2002) A review of twentieth-century drought indices used in the United States. Bull Am Meteorol Soc 83:1149–1166
24. Hong X, Guo S, Zhou Y, Xiong L (2015) Uncertainties in assessing hydrological drought using streamflow drought index for the upper Yangtze River basin. Stoch Environ Res Risk Assess 29:1235–1247
25. Huang S, Huang Q, Chang J, Leng G, Xing L (2015) The response of agricultural drought to meteorological drought and the influencing factors: a case study in the Wei River Basin, China. Agric Water Manag 159:45–54
26. Humphries P, Baldwin DS (2003) Drought and aquatic ecosystems: an introduction. Freshw Biol 48:1141–1146
27. Liu M, Li S, Wu J, He H, Huang H, Lü A (2015) Change of drought and its impact on potential yield of wheat in agricultural region of Shan-Gan-Ning region in 19612010. Trans Chin Soc Agric Eng 31:147–154
28. Mallya G, Zhao L, Song XC, Niyogi D, Govindaraju RS (2013) 2012 Midwest drought in the United States. J Hydrol Eng 18:737–745
29. McKee TB (1995) Drought monitoring with multiple time scales, in: Proceedings of 9th Conference on Applied Climatology, Boston, 1995
30. McKee TB, Doesken NJ, Kleist J, others (1993) The relationship of drought frequency and duration to time scales, in: Proceedings of the 8th Conference on Applied Climatology. pp. 179–183
31. Milly PCD, Wetherald RT, Dunne KA, Delworth TL (2002) Increasing risk of great floods in a changing climate. Nature 415:514–517
32. Mishra AK, Singh VP (2010) A review of drought concepts. J Hydrol 391:202–216
33. Monteith JL (1965) Evaporation and environment. Symposia of the society for experimental biology,205–234
34. Moriasi DN, Arnold JG, Van Liew MW, Bingner RL, Harmel RD, Veith TL (2007) Model evaluation guidelines for systematic quantification of accuracy in watershed simulations. Transactions of the ASABE, American society of agricultural and biological engineers, 50(3), 885–900
35. Nalbantis I (2008) Evaluation of a hydrological drought index. Eur Water 23:67–77
36. Nalbantis I, Tsakiris G (2009) Assessment of hydrological drought revisited. Water Resour Manag 23:881–897
37. Neitsch S, Arnold J, Kiniry J, Williams J (2011) Soil & Water Assessment Tool Theoretical Documentation Version 2009. Texas Water Resources Institute, pp 1–647

38. Padhiary J, Patra KC, Dash SS, Uday Kumar A (2020) Climate change impact assessment on hydrological fluxes based on ensemble GCM outputs: a case study in eastern Indian River Basin. J Water Clim 11(4):1676–1694
39. Peña-Gallardo M, Vicente-Serrano SM, Quiring S, Svoboda M, Hannaford J, Tomas-Burguera M, Martín-Hernández N, Domínguez-Castro F, Kenawy E, A (2019) Response of crop yield to different time-scales of drought in the United States: Spatio-temporal patterns and climatic and environmental drivers. Agric For Meteorol 264:40–55
40. Quiring SM, Ganesh S (2010) Evaluating the utility of the Vegetation Condition Index (VCI) for monitoring meteorological drought in Texas. Agric For Meteorol 150:330–339
41. Shafer BA (1982) Developemnet of a surface water supply index (SWSI) to assess the severity of drought conditions in snowpack runoff areas, in: Proceedings of the 50th Annual Western Snow Conference, Colorado State University, Fort Collins, 1982
42. Sheffield J, Wood EF, Roderick ML (2012) Little change in global drought over the past 60 years. Nature 491:435–438
43. Shukla S, Wood AW (2008) Use of a standardized runoff index for characterizing hydrologic drought.Geophys. Res. Lett.35
44. Smakhtin VU (2001) Low flow hydrology: a review. J Hydrol 240:147–186
45. Smith M (1992) CROPWAT: A computer program for irrigation planning and management. Food \& Agriculture Org
46. Sperber KR, Annamalai H, Kang I-S, Kitoh A, Moise A, Turner A, Wang B, Zhou T (2013) The Asian summer monsoon: an intercomparison of CMIP5 vs. CMIP3 simulations of the late 20th century. Clim. Dyn., Springer, 41(9–10), 2711–2744
47. Teutschbein C, Seibert J (2013) Is bias correction of regional climate model (RCM) simulations possible for nonstationary conditions. Hydrol Earth Syst Sci 17:5061–5077
48. Tigkas D, Tsakiris G (2015) Early estimation of drought impacts on rainfed wheat yield in Mediterranean climate. Environ Process 2(1):97–114
49. Tran LT, O'Neill RV, Bruins RJF, Smith ER, Harden C (2015) Linking land use/land cover with climatic and geomorphologic factors in regional mean annual streamflow models with geospatial regression approach. Prog Phys Geogr 39:258–274
50. Tsakiris G, Pangalou D, Vangelis H (2007) Regional drought assessment based on the Reconnaissance Drought Index (RDI). Water Resour Manag 21:821–833
51. Van Rooy MP (1965) A rainfall anomally index independent of time and space. notos
52. Vicente-Serrano SM, Beguer\'\ia S, López-Moreno JI (2010) A multiscalar drought index sensitive to global warming: the standardized precipitation evapotranspiration index. J Clim 23:1696–1718
53. Wang H, Vicente-Serrano SM, Tao F, Zhang X, Wang P, Zhang C, Chen Y, Zhu D, El Kenawy A (2016) Monitoring winter wheat drought threat in Northern China using multiple climate-based drought indices and soil moisture during 2000–2013. Agric For Meteorol 228:1–12
54. Wilk J, Hughes DA (2002) Simulating the impacts of land-use and climate change on water resource availability for a large south Indian catchment. Hydrol Sci J 47(1):19–30
55. Zhang L, Nan Z, Yu W, Ge Y (2016) Hydrological responses to land-use change scenarios under constant and changed climatic conditions. Environ Manage 57:412–431

Figures

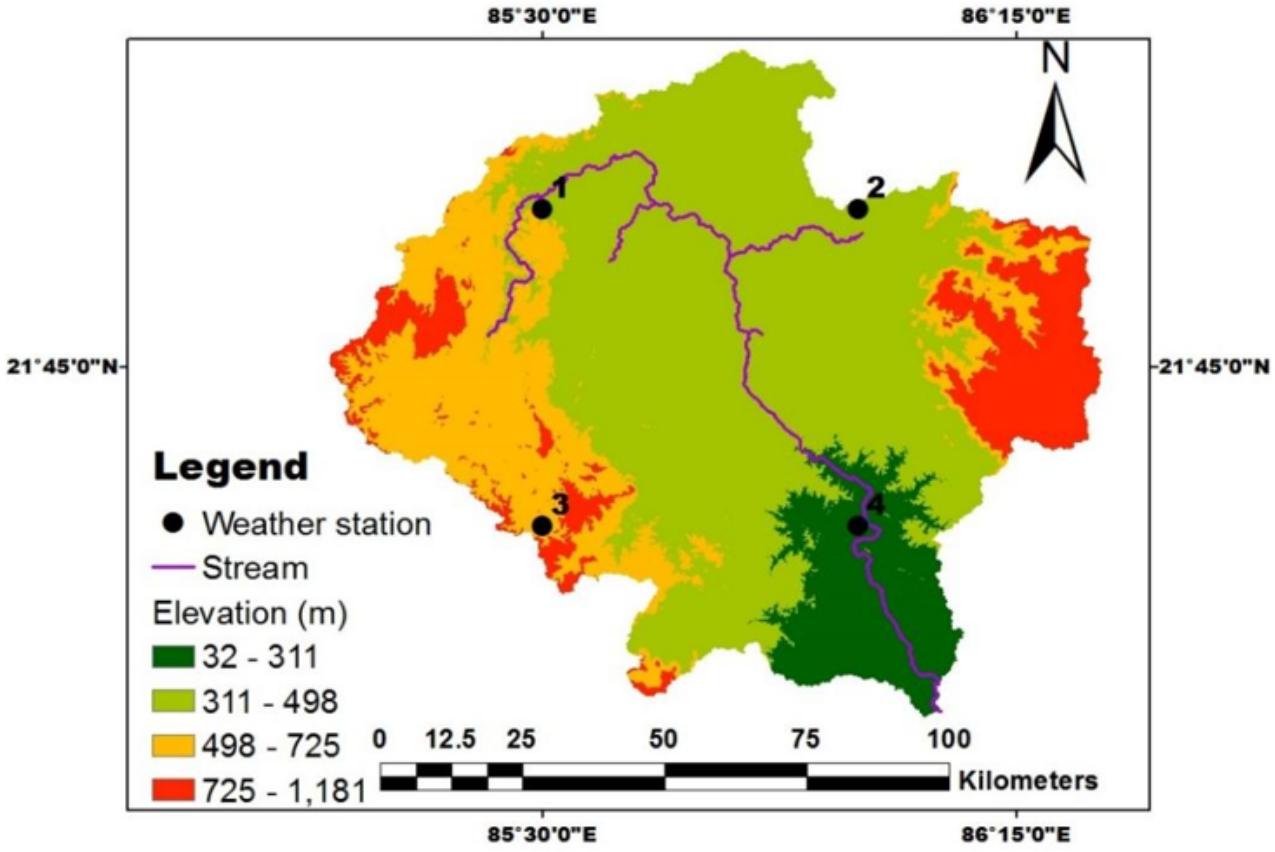

Figure 1

Location of the study area.

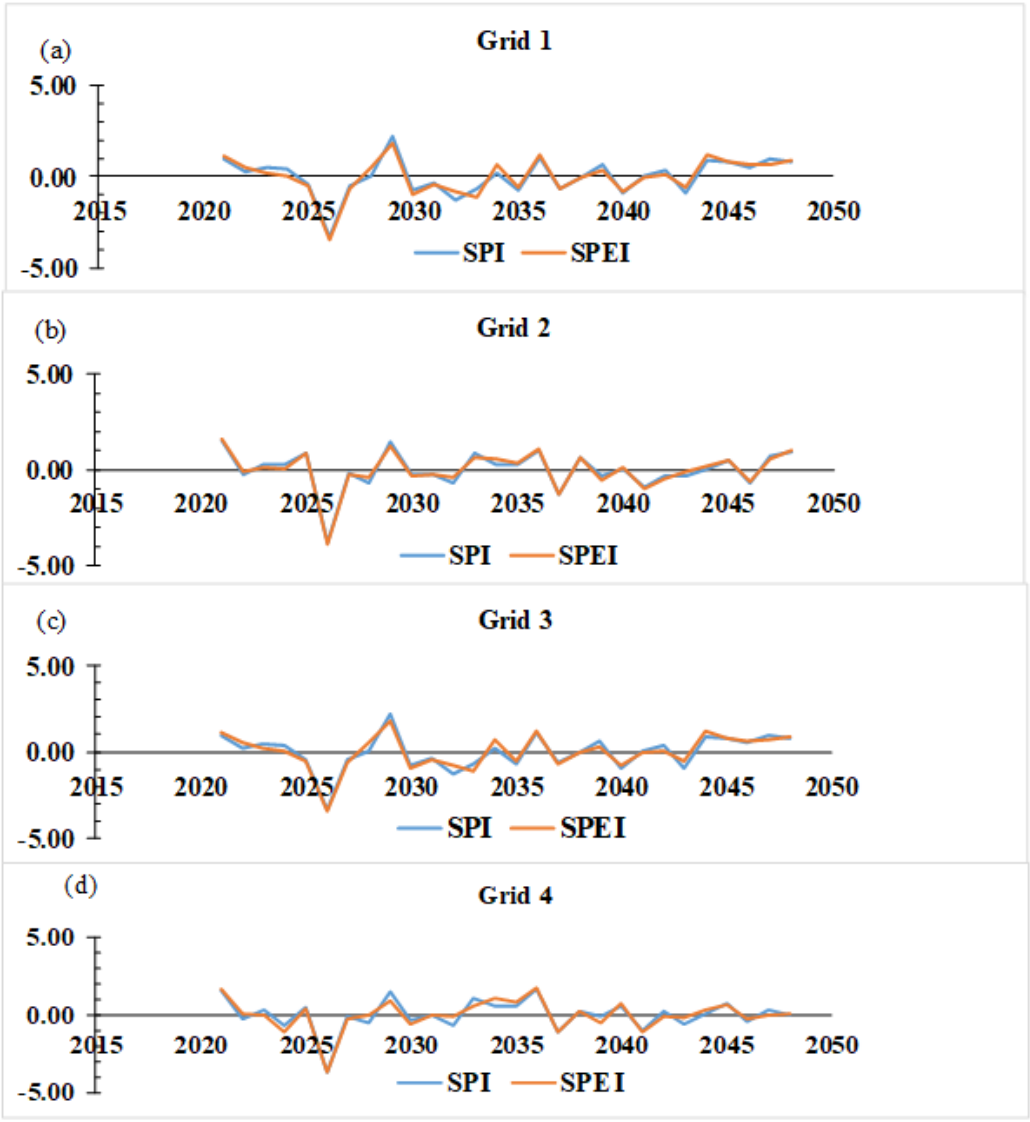

Figure 2

Annual variation of SPI and SPEI in the catchment for future periods (2021-2050).

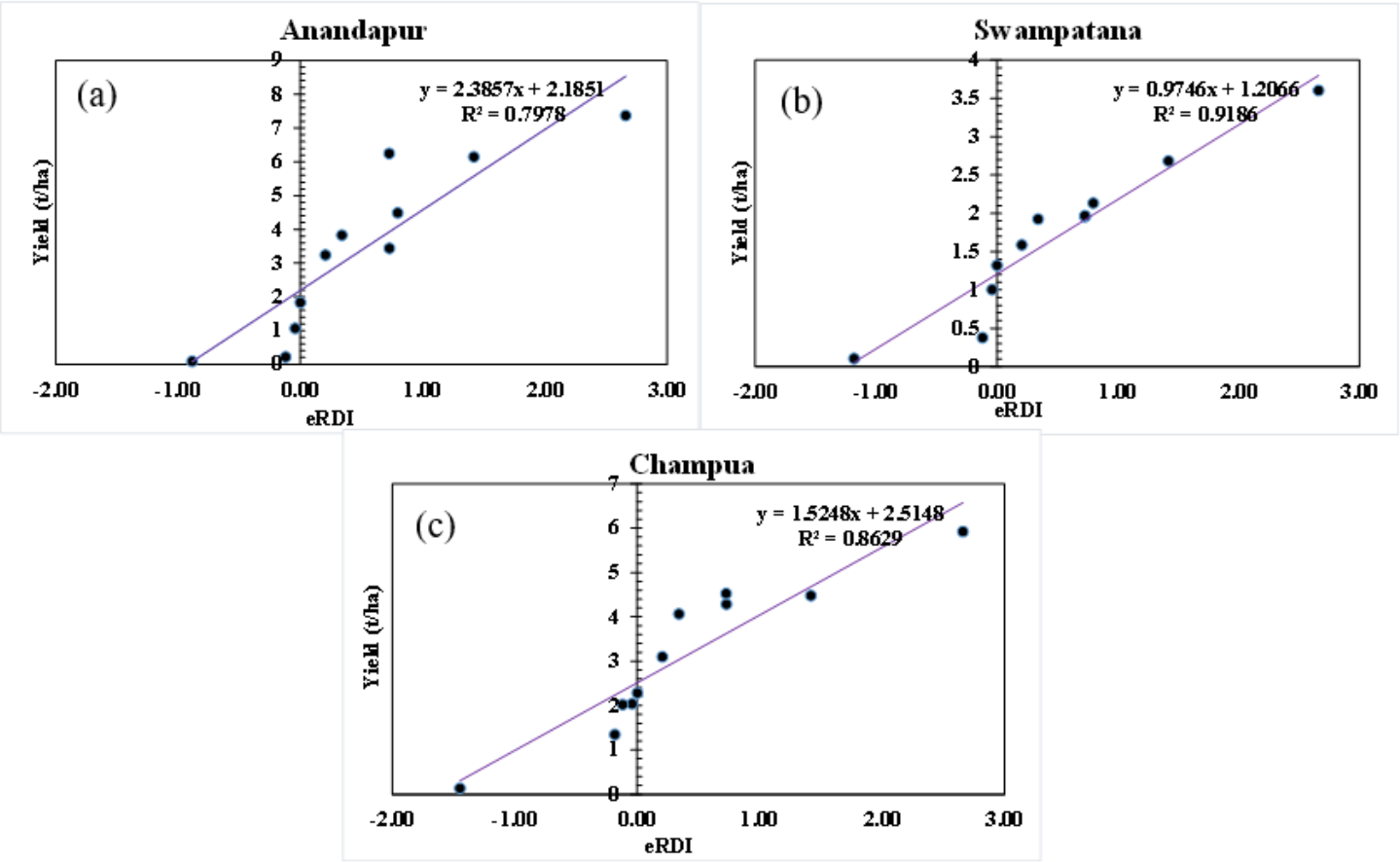

Figure 3

Scatter plot for crop yield variability against the 6-month aSPEI values.

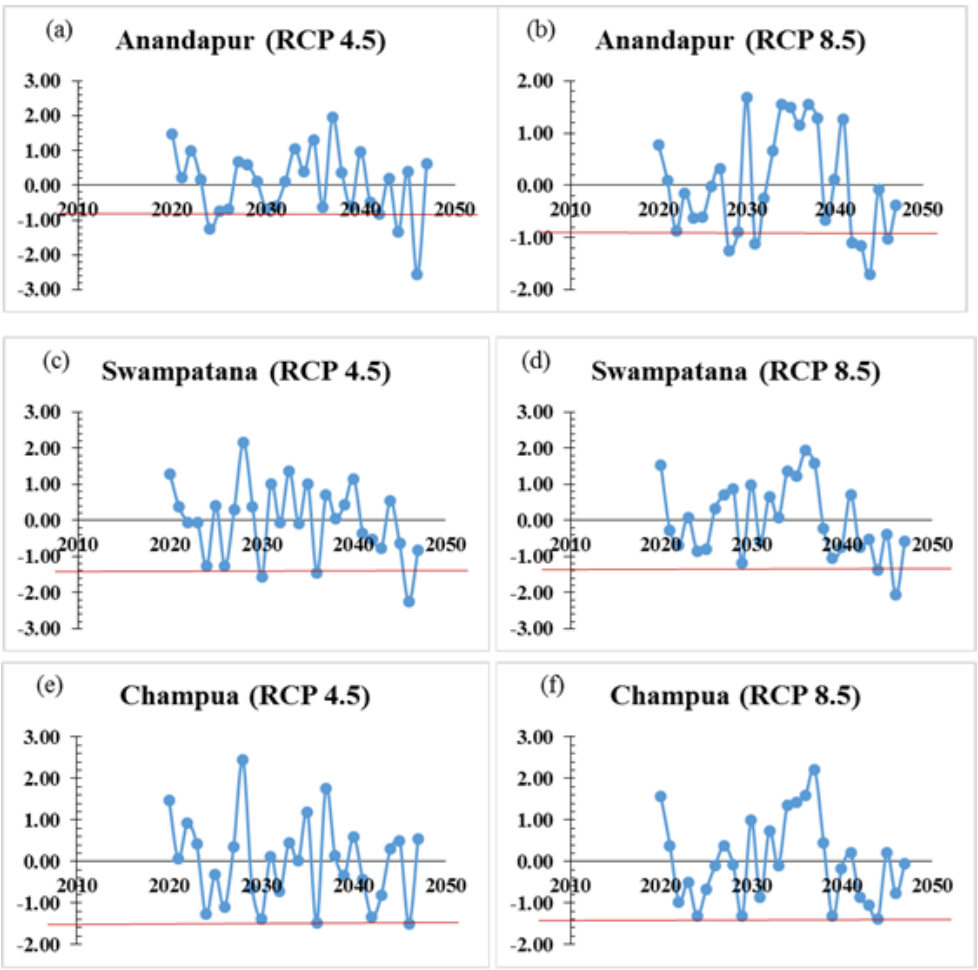

Figure 4

Identification of future drought events that reduces crop yield for the three specified districts. The red line represents the critical point of aSPEI (aSPEIc), below which that climatic factors significantly decrease crop yield.

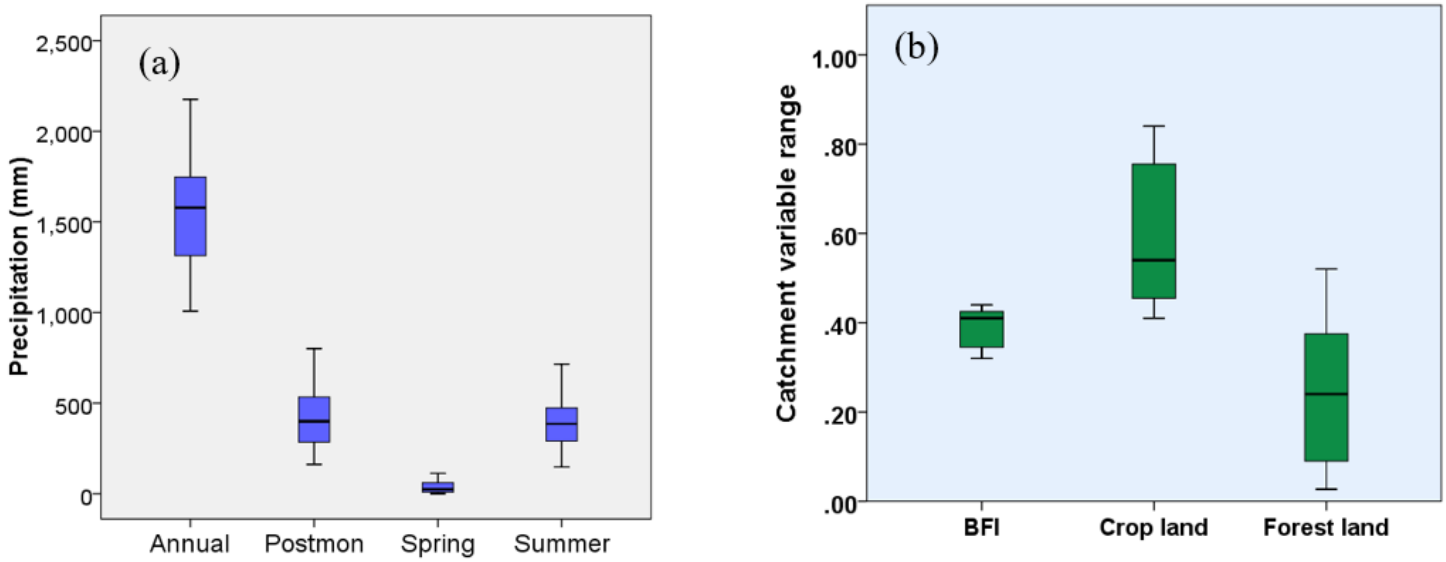

Figure 5

Variation in the climate and catchment variables in the study catchment.